SLAC-PUB-7129
UCSD-96-05
March 1996
hep-ph/9603400

Hadro-production of Quarkonia in Fixed Target Experiments*

M. Beneke[1] and I.Z. Rothstein[2]

[1]*Stanford Linear Accelerator Center,*
Stanford Univerity, Stanford, CA 94309, U.S.A.

[2]*University of California, San Diego,*
9500 Gilman Drive, La Jolla, CA 92093, U.S.A.

Abstract

We analyze charmonium and bottomonium production at fixed target experiments. We find that inclusion of color octet production channels removes large discrepancies between experiment and the predictions of the color singlet model for the total production cross section. Furthermore, including octet contributions accounts for the observed direct to total J/ψ production ratio. As found earlier for photo-production of quarkonia, a fit to fixed target data requires smaller color octet matrix elements than those extracted from high-p_t production at the Tevatron. We argue that this difference can be explained by systematic differences in the velocity expansion for collider and fixed-target predictions. While the color octet mechanism thus appears to be an essential part of a satisfactory description of fixed target data, important discrepancies remain for the χ_{c1}/χ_{c2} production ratio and J/ψ (ψ') polarization. These discrepancies, as well as, the differences between pion and proton induced collisions emphasize the need for including higher twist effects in addition to the color octet mechanism.

PACS numbers: 13.85.Ni, 13.88.+e, 14.40.Gx

* Research supported by the Department of Energy under contract DE-AC03-76SF00515.

1 Introduction

Quarkonium production has traditionally been calculated in the color singlet model (CSM) [1]. Although the model successfully describes the production rates for some quarkonium states, it has become clear that it fails to provide a theoretically and phenomenologically consistent picture of all production processes. In hadroproduction of charmonia at fixed target energies ($\sqrt{s} < 50$ GeV), the ratio of the number of J/ψ produced directly to those arising from decays of higher charmonium states is under-predicted by at least a factor five [2]. The χ_{c1} to χ_{c2} production ratio is far too low, and the observation of essentially unpolarized J/ψ and ψ' can not be reproduced. At Tevatron collider energies, when fragmentation production dominates, the deficit of direct J/ψ and ψ' in the color singlet model is even larger. This deficit has been referred to as the 'ψ'-anomaly' [3, 4].

These discrepancies suggest that the color singlet model is too restrictive and that other production mechanisms are necessitated. Indeed, the CSM requires that the quark-antiquark pair that binds into a quarkonium state be produced on the time scale $\tau \simeq 1/m_Q$ with the same color and angular momentum quantum numbers as the eventually formed quarkonium. Consequently, a hard gluon has to be emitted to produce a ${}^3S_1$ state in the CSM and costs one power of α_s/π. Since the time scale for quarkonium formation is of order $1/(m_Q v^2)$, where v is the relative quark-antiquark velocity in the quarkonium bound state, this suppression can be overcome if one allows for the possibility that the quark-antiquark pair is in any angular momentum or color state when produced on time scales $\tau \simeq 1/m_Q$. Subsequent evolution into the physical quarkonium state is mediated by emission of soft gluons with momenta of order $m_Q v^2$. Since the quark-antiquark pair is small in size, the emission of these gluons can be analyzed within a multipole expansion. A rigorous formulation [5] of this picture can be given in terms of non-relativistic QCD (NRQCD). Accordingly, the production cross section for a quarkonium state H in the process

$$A + B \longrightarrow H + X, \tag{1}$$

can be written as

$$\sigma_H = \sum_{i,j} \int_0^1 dx_1 dx_2 \, f_{i/A}(x_1) f_{j/B}(x_2) \, \hat{\sigma}(ij \to H) \,, \tag{2}$$

$$\hat{\sigma}(ij \to H) = \sum_n C^{ij}_{\bar{Q}Q[n]} \langle \mathcal{O}^H_n \rangle \,. \tag{3}$$

Here the first sum extends over all partons in the colliding hadrons and $f_{i/A}$ etc. denote the corresponding distribution functions. The short-distance ($x \sim 1/m_Q \gg 1/(m_Q v)$) coefficients $C^{ij}_{\bar{Q}Q[n]}$ describe the production of a quark-antiquark pair in a state n and have expansions in $\alpha_s(2m_Q)$. The parameters[†] $\langle \mathcal{O}^H_n \rangle$ describe the subsequent hadronization of the $Q\bar{Q}$ pair into a jet containing the quarkonium H and light hadrons. These matrix elements can not be computed perturbatively, but their relative importance in powers of v can be estimated from the selection rules for multipole transitions.

[†]Their precise definition is given in Sect. VI of [5].

The color octet picture has led to the most plausible explanation of the 'ψ'-anomaly' and the direct J/ψ production deficit. In this picture gluons fragment into quark-antiquark pairs in a color-octet ${}^3S_1^{(8)}$ state which then hadronizes into a ψ' (or J/ψ) [6, 7, 8]. Aside from this striking prediction, the color octet mechanism remains largely untested. Its verification now requires considering quarkonium production in other processes in order to demonstrate the process-independence (universality) of the production matrix elements $\langle \mathcal{O}_n^H \rangle$, which is an essential prediction of the factorization formula (3).

Direct J/ψ and ψ' production at large $p_t \gg 2m_Q$ (where m_Q denotes the heavy *quark* mass) is rather unique in that a single term, proportional to $\langle \mathcal{O}_8^H({}^3S_1) \rangle$, overwhelmingly dominates the sum (3). On the other hand, in quarkonium formation at moderate $p_t \sim 2m_Q$ at colliders and in photo-production or fixed target experiments ($p_t \sim 1\,\mathrm{GeV}$), the signatures of color octet production are less dramatic, because they are not as enhanced by powers of π/α_s or p_t^2/m_Q^2 over the singlet mechanisms. Furthermore, theoretical predictions are parameterized by more unknown octet matrix elements and are afflicted by larger uncertainties. In particular, there are large uncertainties due to the increased sensitivity to the heavy quark mass close to threshold. (The production of a quark-antiquark pair close to threshold is favored by the rise of parton densities at small x.) These facts complicate establishing color octet mechanisms precisely in those processes where experimental data is most abundant.

Cho and Leibovich [9] studied direct quarkonium production at moderate p_t at the Tevatron collider and were able to extract a value for a certain combination of unknown parameters $\langle \mathcal{O}_8^H({}^1S_0) \rangle$ and $\langle \mathcal{O}_8^H({}^3P_0) \rangle$ ($H = J/\psi, \psi', \Upsilon(1S), \Upsilon(2S)$). A first test of universality comes from photo-production [10, 11, 12], where a different combination of these two matrix elements becomes important near the elastic peak at $z \approx 1$, where $z = p \cdot k_\psi / p \cdot k_\gamma$, and p is the proton momentum. A fit to photo-production data requires much smaller matrix elements than those found in [9]. Taken at face value, this comparison would imply failure of the universality assumption underlying the non-relativistic QCD approach. However, the extraction from photo-production should be regarded with caution since the NRQCD formalism describes inclusive quarkonium production only after sufficient smearing in z and is not applicable in the exclusive region close to $z = 1$, where diffractive quarkonium production is important.

In this paper we investigate the universality of the color octet quarkonium production matrix elements in fixed target hadron collisions and re-evaluate the failures of the CSM in fixed target production [2] after inclusion of color octet mechanisms. Some of the issues involved have already been addressed by Tang and Vänttinen [13] and by Gupta and Sridhar [14], but a complete survey is still missing. We also differ from [13] in the treatment of polarized quarkonium production and the assessment of the importance of color octet contributions and from [14] in the color octet short-distance coefficients.

The paper is organized as follows: In Sect. 2 we compile the leading order color singlet and color octet contributions to the production rates for ψ', χ_J, J/ψ as well as bottomonium. In Sect. 3 we present our numerical results for proton and pion induced collisions. Sect. 4 is devoted to the treatment of polarized quarkonium production. As polarization remains one of the cleanest tests of octet quarkonium production at large p_t [15, 16], we clarify in detail the conflicting treatments of polarized production in [16] and [9]. Sect. 5 is dedicated to a comparison of the extracted color-octet matrix elements from fixed target experiments with those from photo-production and the Tevatron. We argue that kinematical effects and small-x

effects can bias the extraction of NRQCD matrix elements so that a fit to Tevatron data at large p_t requires larger matrix elements than the fit to fixed target and photo-production data. The final section summarizes our conclusions.

2 Quarkonium production cross sections at fixed target energies

2.1 Cross sections

We begin with the production cross section for ψ' which does not receive contributions from radiative decays of higher charmonium states. The $2 \to 2$ parton diagrams produce a quark-antiquark pair in a color-octet state or P-wave singlet state (not relevant to ψ') and therefore contribute to ψ' production at order $\alpha_s^2 v^7$. (For charmonium $v^2 \approx 0.25 - 0.3$, for bottomonium $v^2 \approx 0.08 - 0.1$.) The $2 \to 3$ parton processes contribute to the color singlet processes at order $\alpha_s^3 v^3$. Using the notation in (2):

$$\begin{aligned}\hat{\sigma}(gg \to \psi') &= \frac{5\pi^3\alpha_s^2}{12(2m_c)^3 s}\,\delta(x_1x_2 - 4m_c^2/s)\left[\langle \mathcal{O}_8^{\psi'}(^1S_0)\rangle + \frac{3}{m_c^2}\langle \mathcal{O}_8^{\psi'}(^3P_0)\rangle + \frac{4}{5m_c^2}\langle \mathcal{O}_8^{\psi'}(^3P_2)\rangle\right] \\ &\quad + \frac{20\pi^2\alpha_s^3}{81(2m_c)^5}\,\Theta(x_1x_2 - 4m_c^2/s)\,\langle \mathcal{O}_1^{\psi'}(^3S_1)\rangle\, z^2\left[\frac{1-z^2+2z\ln z}{(1-z)^2} + \frac{1-z^2-2z\ln z}{(1+z)^3}\right] \quad (4)\end{aligned}$$

$$\hat{\sigma}(gq \to \psi') = 0 \quad (5)$$

$$\hat{\sigma}(q\bar{q} \to \psi') = \frac{16\pi^3\alpha_s^2}{27(2m_c)^3 s}\,\delta(x_1x_2 - 4m_c^2/s)\,\langle \mathcal{O}_8^{\psi'}(^3S_1)\rangle \quad (6)$$

Here $z \equiv (2m_c)^2/(s x_1 x_2)$, $\sqrt{s}$ is the center-of-mass energy and α_s is normalized at the scale $2m_c$. Corrections to these cross sections are suppressed by either α_s/π or v^2. Note that the relativistic corrections to the color singlet cross section are substantial in specific kinematic regions $z \to 0, 1$ [17]. For $\sqrt{s} > 15\,\mathrm{GeV}$ these corrections affect the total cross section by less than 50% and decrease as the energy is raised [1]. Furthermore, notice that we have expressed the short-distance coefficients in terms of the charm quark mass, $M_{\psi'} \approx 2m_c$, rather than the true ψ' mass. Although the difference is formally of higher order in v^2, this choice is conceptually favored since the short-distance coefficients depend only on the physics prior to quarkonium formation. All quarkonium specific properties which can affect the cross section, such as quarkonium mass differences, are hidden in the matrix elements.

The production of P-wave quarkonia differs from S-waves since color singlet and color octet processes enter at the same order in v^2 as well as α_s in general. An exception is χ_{c1}, which can not be produced in $2 \to 2$ parton reactions through gluon-gluon fusion in a color singlet state. Since at order α_s^2, the χ_{c1} would be produced only in a $q\bar{q}$ collision, we also include the gluon fusion diagrams at order α_s^3, which are enhanced by the gluon distribution. We have for χ_{c0},

$$\hat{\sigma}(gg \to \chi_{c0}) = \frac{2\pi^3\alpha_s^2}{3(2m_c)^3 s}\,\delta(x_1x_2 - 4m_c^2/s)\frac{1}{m_c^2}\langle \mathcal{O}_1^{\chi_{c0}}(^3P_0)\rangle \quad (7)$$

$$\hat{\sigma}(gq \to \chi_{c0}) = 0 \tag{8}$$

$$\hat{\sigma}(q\bar{q} \to \chi_{c0}) = \frac{16\pi^3\alpha_s^2}{27(2m_c)^3 s}\,\delta(x_1x_2 - 4m_c^2/s)\,\langle \mathcal{O}_8^{\chi_{c0}}(^3S_1)\rangle\,, \tag{9}$$

for χ_{c1},

$$\begin{aligned}\hat{\sigma}(gg \to \chi_{c1}) &= \frac{2\pi^2\alpha_s^3}{9(2m_c)^5}\,\Theta(x_1x_2 - 4m_c^2/s)\frac{1}{m_c^2}\langle \mathcal{O}_1^{\chi_{c1}}(^3P_1)\rangle \\ &\times\left[\frac{4z^2\ln z\,(z^8+9z^7+26z^6+28z^5+17z^4+7z^3-40z^2-4z-4}{(1+z)^5(1-z)^4}\right. \\ &\left.+\frac{z^9+39z^8+145z^7+251z^6+119z^5-153z^4-17z^3-147z^2-8z+10}{3(1-z)^3(1+z)^4}\right]\end{aligned} \tag{10}$$

$$\hat{\sigma}(gq \to \chi_{c1}) = \frac{8\pi^2\alpha_s^3}{81(2m_c)^5}\,\Theta(x_1x_2 - 4m_c^2/s)\frac{1}{m_c^2}\langle \mathcal{O}_1^{\chi_{c1}}(^3P_1)\rangle\left[-z^2\ln z + \frac{4z^3-9z+5}{3}\right]$$

$$\hat{\sigma}(q\bar{q} \to \chi_{c1}) = \frac{16\pi^3\alpha_s^2}{27(2m_c)^3 s}\,\delta(x_1x_2 - 4m_c^2/s)\,\langle \mathcal{O}_8^{\chi_{c1}}(^3S_1)\rangle\,, \tag{11}$$

and for χ_{c2}

$$\hat{\sigma}(gg \to \chi_{c2}) = \frac{8\pi^3\alpha_s^2}{45(2m_c)^3 s}\,\delta(x_1x_2 - 4m_c^2/s)\frac{1}{m_c^2}\langle \mathcal{O}_1^{\chi_{c2}}(^3P_2)\rangle \tag{12}$$

$$\hat{\sigma}(gq \to \chi_{c2}) = 0 \tag{13}$$

$$\hat{\sigma}(q\bar{q} \to \chi_{c2}) = \frac{16\pi^3\alpha_s^2}{27(2m_c)^3 s}\,\delta(x_1x_2 - 4m_c^2/s)\,\langle \mathcal{O}_8^{\chi_{c2}}(^3S_1)\rangle\,. \tag{14}$$

Note that in the NRQCD formalism the infrared sensitive contributions to the $q\bar{q}$-induced color-singlet process at order α_s^3 are factorized into the color octet matrix elements $\langle \mathcal{O}_8^{\chi_{cJ}}(^3S_1)\rangle$, so that the $q\bar{q}$ reactions at order α_s^3 are truly suppressed by α_s. The production of P-wave states through octet quark-antiquark pairs in a state other than $^3S_1$ is higher order in v^2.

Taking into account indirect production of J/ψ from decays of ψ' and χ_{cJ} states, the J/ψ cross section is given by

$$\sigma_{J/\psi} = \sigma(J/\psi)_{dir} + \sum_{J=0,1,2}\mathrm{Br}(\chi_{cJ} \to J/\psi X)\,\sigma_{\chi_{cJ}} + \mathrm{Br}(\psi' \to J/\psi X)\,\sigma_{\psi'}\,, \tag{15}$$

where 'Br' denotes the corresponding branching fraction and the direct J/ψ production cross section $\sigma(J/\psi)_{dir}$ differs from $\sigma_{\psi'}$ (see (4)) only by the replacement of ψ' matrix elements with J/ψ matrix elements. Finally, we note that charmonium production through B decays is comparatively negligible at fixed target energies.

The $2 \to 2$ parton processes contribute only to quarkonium production at zero transverse momentum with respect to the beam axis. The transverse momentum distribution of H in reaction (1) is not calculable in the $p_t < \Lambda_{QCD}$ region, but the total cross section (which

averages over all p_t) is predicted even if the underlying parton process is strongly peaked at zero p_t.

The transcription of the above formulae to bottomonium production is straightforward. Since more bottomonium states exist below the open bottom threshold than for the charmonium system, a larger chain of cascade decays in the bottomonium system must be included. In particular, there is indirect evidence from $\Upsilon(3S)$ production both at the Tevatron [18] as well as in fixed target experiments (to be discussed below) that there exist yet unobserved $\chi_b(3P)$ states below threshold whose decay into lower bottomonium states should also be included. Our numerical results do not include indirect contributions from potential D-wave states below threshold.

All color singlet cross sections compiled in this section have been taken from the review [1]. We have checked that the color octet short-distance coefficients agree with those given in [9], but disagree with those that enter the numerical analysis of fixed target data in [14].

2.2 Matrix elements

The number of independent matrix elements can be reduced by using the spin symmetry relations

$$\begin{aligned}
\langle \mathcal{O}_1^{\chi_{cJ}}(^3P_J)\rangle &= (2J+1)\,\langle \mathcal{O}_1^{\chi_{c0}}(^3P_0)\rangle \\
\langle \mathcal{O}_8^{\psi}(^3P_J)\rangle &= (2J+1)\,\langle \mathcal{O}_8^{\psi}(^3P_0)\rangle \\
\langle \mathcal{O}_8^{\chi_{cJ}}(^3S_1)\rangle &= (2J+1)\,\langle \mathcal{O}_1^{\chi_{c0}}(^3S_1)\rangle
\end{aligned} \tag{16}$$

and are accurate up to corrections of order v^2 ($\psi = J/\psi, \psi'$ – identical relations hold for bottomonium). This implies that at lowest order in α_s, the matrix elements $\langle \mathcal{O}_8^H(^1S_0)\rangle$ and $\langle \mathcal{O}_8^H(^3P_0)\rangle$ enter fixed target production of J/ψ and ψ' only in the combination

$$\Delta_8(H) \equiv \langle \mathcal{O}_8^H(^1S_0)\rangle + \frac{7}{m_Q^2}\langle \mathcal{O}_8^H(^3P_0)\rangle\,. \tag{17}$$

Up to corrections in v^2, all relevant color singlet production matrix elements are related to radial quarkonium wave functions at the origin and their derivatives by

$$\langle \mathcal{O}_1^H(^3S_1)\rangle = \frac{9}{2\pi}|R(0)|^2 \qquad \langle \mathcal{O}_1^H(^3P_0)\rangle = \frac{9}{2\pi}|R'(0)|^2. \tag{18}$$

We are then left with three non-perturbative parameters for the direct production of each S-wave quarkonium and two parameters for P-states.

The values for these parameters, which we will use below, are summarized in tables 1 and 2. Many of the octet matrix elements, especially for bottomonia, are not established and should be viewed as guesses. The numbers given in the tables are motivated as follows: All color singlet matrix elements are computed from the wavefunctions in the Buchmüller-Tye potential tabulated in [19] and using (18). Similar results within ±30% could be obtained from leptonic and hadronic decays of quarkonia for some of the states listed in the tables. The matrix elements $\langle \mathcal{O}_8^H(^3S_1)\rangle$ are taken from the fits to Tevatron data in [9] with the exception of the $3S$ and $3P$ bottomonium states. In this case, we have chosen the numbers by (rather ad

ME	J/ψ	ψ'	$\Upsilon(1S)$	$\Upsilon(2S)$	$\Upsilon(3S)$
$\langle \mathcal{O}_1^H(^3S_1)\rangle$	1.16	0.76	9.28	4.63	3.54
$\langle \mathcal{O}_8^H(^3S_1)\rangle$	$6.6 \cdot 10^{-3}$	$4.6 \cdot 10^{-3}$	$5.9 \cdot 10^{-3}$	$4.1 \cdot 10^{-3}$	$3.5 \cdot 10^{-3}$
$\Delta_8(H)$	fitted	fitted	$5.0 \cdot 10^{-2}$	$3.0 \cdot 10^{-2}$	$2.3 \cdot 10^{-2}$

Table 1: Matrix elements (ME) for the direct production of a S-wave quarkonium H. All values in GeV^3.

ME	χ_{c0}	$\chi_{b0}(1P)$	$\chi_{b0}(2P)$	$\chi_{b0}(3P)$
$\langle \mathcal{O}_1^H(^3P_0)\rangle/m_Q^2$	$4.4 \cdot 10^{-2}$	$8.5 \cdot 10^{-2}$	$9.9 \cdot 10^{-2}$	0.11
$\langle \mathcal{O}_8^H(^3S_1)\rangle$	$3.2 \cdot 10^{-3}$	0.42	0.32	0.25

Table 2: Matrix elements (ME) for the direct production of a P-wave quarkonium H. All values in GeV^3.

hoc) extrapolation from the $1S$, $2S$ and $1P$, $2P$ states. The combination of matrix elements $\Delta_8(H)$ turns out to be the single most important parameter for direct production of J/ψ and ψ'. For this reason, we leave it as a parameter to be fitted and later compared with constraints available from Tevatron data. For bottomonia we adopt a different strategy since $\Delta_8(H)$ is of no importance for the total (direct plus indirect) bottomonium cross section. We therefore fixed its value using the results of [9] together with some assumption on the relative size of $\langle \mathcal{O}_8^H(^1S_0)\rangle$ and $\langle \mathcal{O}_8^H(^3P_0)\rangle$ and an ad hoc extrapolation for the $3S$ state. Setting $\Delta_8(H)$ to zero for bottomonia would change the cross section by a negligible amount.

3 Results

Figs. 1 to 6 and table 3 summarize our results for the charmonium and bottomonium production cross sections. We use the CTEQ3 LO [20] parameterization for the parton distributions of the protons and the GRV LO [21] parameterization for pions. The quark masses are fixed to be $m_c = 1.5\,\mathrm{GeV}$ and $m_b = 4.9\,\mathrm{GeV}$, as was done in [9]. The strong coupling is evaluated at the scale $\mu = 2m_Q$ ($Q = b, c$) and chosen to coincide with the value implied by the parameterization of the parton distributions (e.g., $\alpha_s(2m_c) \approx 0.23$ for CTEQ3 LO). We comment on these parameter choices in the discussion below. The experimental data have been taken from the compilation in [1] with the addition of results from [22] and the 800 GeV proton beam at Fermilab [23, 24]. All data have been rescaled to the nuclear dependence $A^{0.92}$ for proton-nucleon collisions and $A^{0.87}$ for pion-nucleon collisions. All cross sections are given for $x_F > 0$ only (i.e. integrated over the forward direction in the cms frame where most of the data has been collected).

3.1 ψ'

The total ψ' production cross section in proton-nucleus collisions is shown in Fig. 1. The color-singlet cross section is seen to be about a factor of two below the data and the fit,

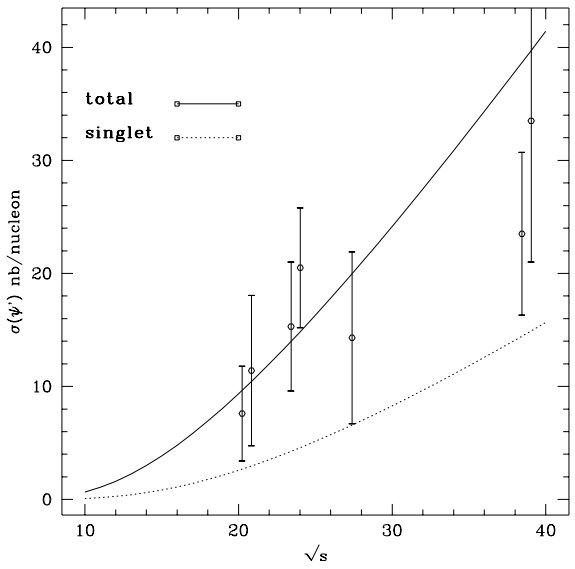

Figure 1: Total (solid) and singlet only (dotted) ψ' production cross section in proton-nucleon collisions ($x_F > 0$ only). The solid line is obtained with $\Delta_8(\psi') = 5.2 \cdot 10^{-3}\,\mathrm{GeV}^3$.

including color octet processes, is obtained with

$$\Delta_8(\psi') = 5.2 \cdot 10^{-3}\,\mathrm{GeV}^3\,. \tag{19}$$

The contribution from $\langle \mathcal{O}_8^{\psi'}(^3S_1)\rangle$ is numerically irrelevant because gluon fusion dominates at all cms energies considered here. The relative magnitude of singlet and octet contributions is consistent with the naive scaling estimate $\pi/\alpha_s \cdot v^4 \approx 1$ (The color singlet cross section acquires an additional suppression, because it vanishes close to threshold when $4m_c^2/(x_1x_2s) \to 1$).

It is important to mention that the color singlet prediction has been expressed in terms of $2m_c = 3\,\mathrm{GeV}$ and not the physical quarkonium mass. Choosing the quarkonium mass reduces the color singlet cross section by a factor of three compared to Fig. 1, leading to an apparent substantial ψ' deficit[‡]. As explained in Sect. 2, choosing quark masses is preferred but leads to large normalization uncertainties due to the poorly known charm quark mass, which could only be partially eliminated if the color singlet wave function were extracted from ψ' decays. If, as in open charm production, a small charm mass were preferred, the data could be reproduced even without a color octet contribution. Although this appears unlikely (see below), we conclude that the total ψ' cross section alone does not provide convincing evidence for the color octet mechanism. If we neglect the color singlet contribution altogether, we obtain $\Delta_8(\psi') < 1.0 \cdot 10^{-2}\,\mathrm{GeV}^3$. This bound is strongly dependent on the value of m_c. Varying m_c between 1.3 GeV and 1.7 GeV changes the total cross section by roughly a factor of eight at $\sqrt{s} = 30\,\mathrm{GeV}$ and even more at smaller $\sqrt{s}$. Compared to this normalization uncertainty, the variation with the choice of parton distribution and $\alpha_s(\mu)$ is negligible. This remark applies to all other charmonium cross sections considered in this section.

[‡]This together with a smaller value for the color singlet radial wavefunction could at least partially explain the huge discrepancy between the CSM and the data that was reported in [23].

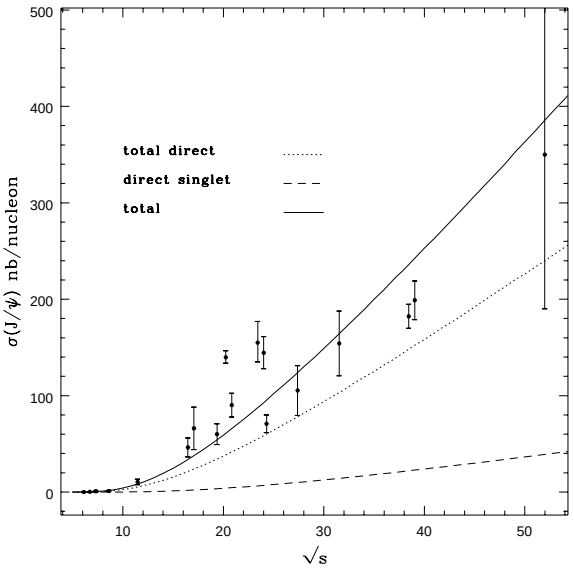

Figure 2: J/ψ production cross sections in proton-nucleon collisions for $x_F > 0$. The dotted line is the direct J/ψ production rate in the CSM and the dashed line includes the contribution from the color-octet processes. The total cross section (solid line) includes radiative feed-down from the χ_{cJ} and ψ' states. The solid line is obtained with $\Delta_8(J/\psi) = 3.0 \cdot 10^{-2}\,\mathrm{GeV}^3$.

3.2 J/ψ

The J/ψ production cross section in proton-nucleon collisions is displayed in Fig. 2. A reasonable fit is obtained for

$$\Delta_8(J/\psi) = 3.0 \cdot 10^{-2}\,\mathrm{GeV}^3\,. \tag{20}$$

We see that the color octet mechanism substantially enhances the direct J/ψ production cross section compared to the CSM, as shown by the dashed and dotted lines in Fig. 2. The total cross section includes feed-down from χ_{cJ} states which is dominated by the color-singlet gluon fusion process. As expected from the cross section in Sect. 2, the largest indirect contribution originates from χ_{c2} states, because χ_{c1} production is suppressed by one power of α_s in the gluon fusion channel. The direct J/ψ production fraction at $\sqrt{s} = 23.7\,\mathrm{GeV}$ ($E = 300\,\mathrm{GeV}$) is 63%, in excellent agreement with the experimental value of 62% [25]. Note that this agreement is not a trivial consequence of fitting the color octet matrix element $\Delta_8(J/\psi)$ to reproduce the observed total cross section since the indirect contribution is dominated by color singlet mechanisms and the singlet matrix elements are fixed in terms of the wavefunctions of [19].

One could ask whether the large sensitivity to the charm quark mass could be exploited to raise the direct production fraction in the CSM, thus obviating the need for octet contributions altogether? As shown in Fig. 3 this is not the case, since the charm mass dependence cancels in the direct-to-total production ratio. It should be mentioned, that expressing all cross sections in terms of the respective quarkonium masses increases $\sigma(J/\psi)_{dir}/\sigma_{J/\psi}$, because $M_{\chi_{cJ}} > M_{J/\psi}$. However, the total color singlet cross section then decreases further and falls short of the data by about a factor five. We therefore consider the the combination of total J/ψ production

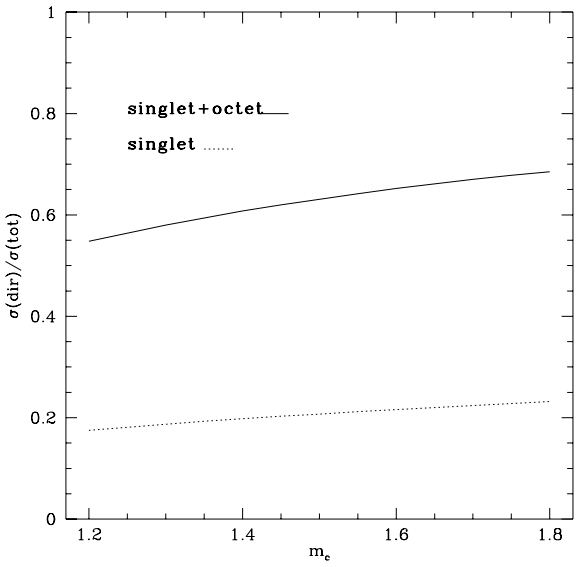

Figure 3: Ratio of direct to total J/ψ production in proton-nucleon collisions as a function of the charm quark mass in the CSM and after inclusion of color octet processes at $E = 300\,\mathrm{GeV}$. The experimental value is 0.62 ± 0.04.

cross section and direct production ratio as convincing evidence for an essential role of color octet mechanisms for direct J/ψ production also at fixed target energies.

The comparison of theoretical predictions with the E705 experiment [25] is summarized in Tab. 3. Including color octet production yields good agreement for direct J/Ψ production, as well as the relative contributions from all χ_{cJ} states and ψ'. Note that the total cross section from [25] is rather large in comparison with other data (see Fig. 2). In the CSM, the direct production cross section of 7 nb should be compared with the measured 89 nb, clearly demonstrating the presence of an additional numerically large production mechanism. Note also that our ψ' cross section in the CSM is rather large in comparison with the direct J/Ψ

	pN th.	pN CSM	pN exp.	$\pi^- N$ th.	$\pi^- N$ CSM	$\pi^- N$ exp.
$\sigma_{J/\psi}$	90 nb	33 nb	143 ± 21 nb	98 nb	38 nb	178 ± 21 nb
$\sigma(J/\psi)_{dir}/\sigma_{J/\psi}$	0.63	0.21	0.62 ± 0.04	0.64	0.24	0.56 ± 0.03
$\sigma_{\psi'}/\sigma(J/\psi)_{dir}$	0.25	0.67	0.21 ± 0.05	0.25	0.66	0.23 ± 0.05
χ-fraction	0.27	0.69	0.31 ± 0.04	0.28	0.66	0.37 ± 0.03
χ_{c1}/χ_{c2} ratio	0.15	0.08	–	0.13	0.11	1.4 ± 0.4

Table 3: Comparison of quarkonium production cross sections in the color singlet model (CSM) and the NRQCD prediction (th.) with experiment at $E = 300$ GeV and $E = 185$ GeV (last line only). The 'χ-fraction' is defined by $\sum_{J=1,2} \mathrm{Br}(\chi_{cJ} \to J/\psi X)\, \sigma_{\chi_{cJ}}/\sigma_{J/\psi}$. The '$\chi_{c1}/\chi_{c2}$'-ratio is defined by $\mathrm{Br}(\chi_{c1} \to J/\psi X)\, \sigma_{\chi_{c1}}/(\mathrm{Br}(\chi_{c2} \to J/\psi X)\, \sigma_{\chi_{c2}})$.

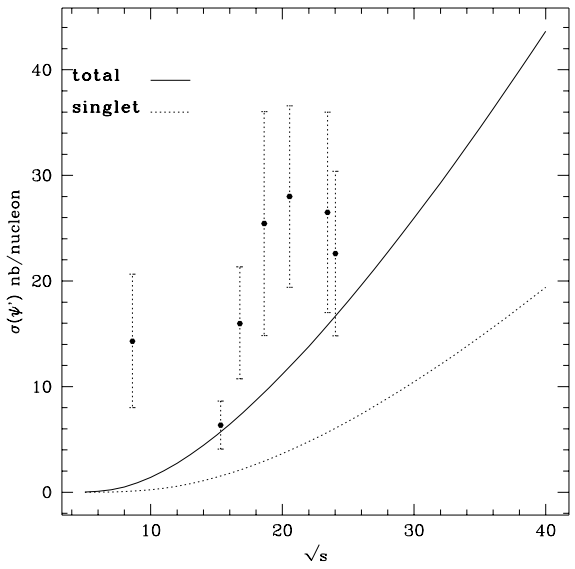

Figure 4: Total (solid) and singlet only (dotted) ψ' production cross section in pion-nucleon collisions ($x_F > 0$ only). The solid line is obtained with $\Delta_8(\psi') = 5.2 \cdot 10^{-3}\,\mathrm{GeV}^3$.

cross section in the CSM. A smaller value which compares more favorably with the data could be obtained if one expressed the cross section in terms of quarkonium masses [2]. From the point of view presented here, this agreement appears coincidental since the cross sections are dominated by octet production.

Perhaps the worst failure of the theory is the χ_{c1} to χ_{c2} ratio in the feed-down contribution that has been measured in the WA11 experiment at $E = 185\,\mathrm{GeV}$ [26]. We see that the prediction is far too small even after inclusion of color octet contributions. The low rate of χ_1 production is due to the fact, as already mentioned, that the gluon-gluon fusion channel is suppressed by α_s/π compared to χ_{c2} due to angular momentum constraints. Together with J/ψ (and ψ') polarization, discussed in Sect. 4, the failure to reproduce this ratio emphasizes the importance of yet other production mechanisms, presumably of higher twist, which are naively suppressed by Λ_{QCD}/m_c [2].

3.3 Pion-induced collisions

The ψ' and J/ψ production cross section in pion-nucleon collisions are shown in Figs. 4 and 5. The discussion for proton-induced collisions applies with little modification to the pion case. A breakdown of contributions to the J/ψ cross section at $E = 300\,\mathrm{GeV}$ is given in table 3. The theoretical prediction is based on the values of $\Delta_8(H)$ extracted from the proton data. Including color octet contributions can add little insight into the question of why the pion-induced cross sections appear to be systematically larger than expected. This issue has been extensively discussed in [1]. The discrepancy may be an indication that, either the gluon distribution in the pion is not really understood (although using parameterizations different from GRV LO tends to yield rather lower theoretical predictions), or that a genuine difference in higher twist effects for the proton and the pion exists.

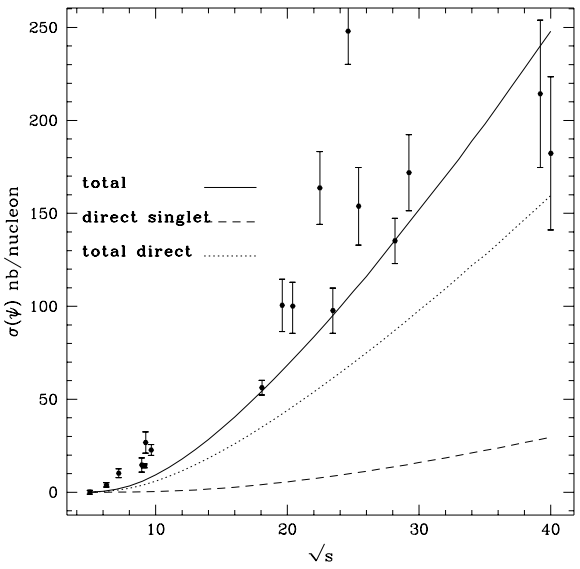

Figure 5: J/ψ production cross sections in pion-nucleon collisions for $x_F > 0$. Direct J/ψ production in the CSM (dashed line) and after inclusion of color-octet processes (dotted line). The total cross section (solid line) includes radiative feed-down from the χ_{cJ} and ψ' states. The solid line is obtained with $\Delta_8(J/\psi) = 3.0 \cdot 10^{-2}\,\mathrm{GeV}^3$.

3.4 $\Upsilon(nS)$

If higher twist effects are important for fixed target charmonium production, their importance should decrease for bottomonium production and facilitate a test of color octet production. Unfortunately, data for bottomonium production at fixed target energies is sparse and does not allow us to complete this test.

Due to the increase of the quark mass, bottomonium production differs in several ways from charmonium production, from a theoretical standpoint. The relative quark-antiquark velocity squared decreases by a factor of three, thus, the color octet contributions to direct production of $\Upsilon(nS)$ are less important since they are suppressed by v^4 (at the same time $\alpha_s(2m_Q)$ decreases much less). The situation is exactly the opposite for the production of P-wave bottomonia. In this case the color singlet and octet contributions scale equally in v^2. The increased quark mass, together with an increased relative importance of the octet matrix element $\langle \mathcal{O}_8^{\chi_{b0}}(^3S_1)\rangle$ (extracted from Tevatron data in [9]) as compared to the singlet wavefunction (compare χ_{c0} with χ_{b0} in Tab. 2), leads to domination of quark-antiquark pair initiated processes. Consequently, the direct $\Upsilon(nS)$ production cross section is at least a factor ten below the indirect contributions from χ_b-decays. This observation leads to the conclusion that the number of $\Upsilon(3S)$ observed by the E772 experiment [27] can only be explained if $\chi_{bJ}(3P)$ states that have not yet been observed directly exist below the open bottom threshold. Such indirect evidence has also been obtained from bottomonium production at the Tevatron collider [18].

To obtain our numerical results shown in Fig. 6, we assumed that these $\chi_{bJ}(3P)$ states decay into $\Upsilon(3S)$ with the same branching fractions as the corresponding $n = 2$ states. The

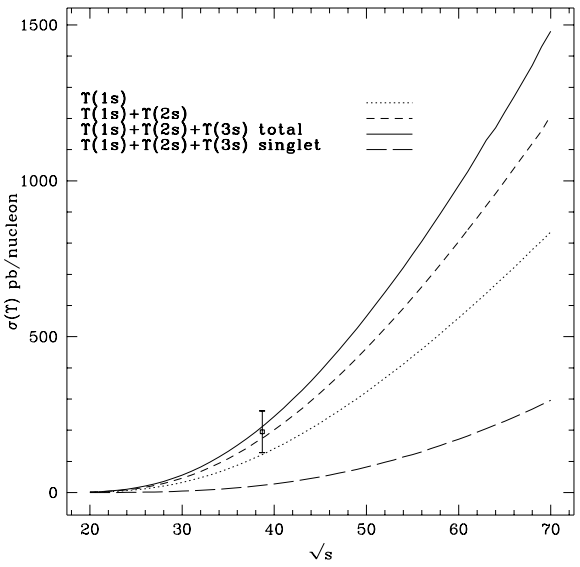

Figure 6: Total (direct plus indirect) $\Upsilon(nS)$ production cross sections (for $x_F > 0$), consecutively summed over n. The data point refers to the sum of $n = 1, 2, 3$.

total cross sections are compared with the experimental value $195 \pm 67\,\mathrm{pb/nucleon}$ obtained from [24] at $E = 800\,\mathrm{GeV}$ for the sum of $\Upsilon(nS)$, $n = 1, 2, 3$ and show very good agreement. The color-singlet processes alone would have led to a nine times smaller prediction at this energy. We should note, however, that integration of the x_F-distribution for $\Upsilon(1S)$ production given in [27] indicates a cross section about two to three times smaller than the central value quoted by [24]. The theoretical prediction for the relative production rates of $\Upsilon(1S) : \Upsilon(2S) : \Upsilon(3S)$ is $1 : 0.42 : 0.30$ to be compared with the experimental ratio [27] $1 : 0.29 : 0.15$[§]. This comparison should not be over interpreted since it depends largely on the rather uncertain octet matrix elements for P-wave bottomonia. Due to lack of more data we also hesitate to use this comparison for a new determination of these matrix elements.

4 ψ' and J/ψ Polarization

In this section, we deal with ψ' and J/ψ polarization at fixed target energies and at colliders at large transverse momentum. Before returning to fixed target production in Sect. 4.2, we digress on large-p_t production. We recall that, at large $p_t^2 \gg 4m_Q^2$, ψ' and direct J/ψ production is dominated by gluon fragmentation into color octet quark-antiquark pairs and expected to yield transversely polarized quarkonia [15]. The reason for this is that a fragmenting gluon can be considered as on-shell and therefore transverse. Due to spin symmetry of NRQCD, the quarkonium inherits the transverse polarization up to corrections of order $4m_c^2/p_T^2$ and v^4. Furthermore, it has been shown [16] that including radiative corrections to gluon fragmentation still leads to more than 90% transversely polarized ψ' (direct J/ψ). Thus, polarization

[§] These numbers were taken from the raw data with no concern regarding the differing efficiencies for the individual states.

provides one of the most significant tests for the color octet production mechanism at large transverse momenta. At moderate $p_t^2 \sim 4m_c^2$, non-fragmentation contributions proportional to $\langle \mathcal{O}_8^H(^1S_0)\rangle$ and $\langle \mathcal{O}_8^H(^3P_J)\rangle$ are sizeable [9]. Understanding their polarization yield quantitatively is very important since most of the p_t-integrated data comes from the lower p_t-region. The calculation of the polarization yield has also been attempted in [9]. However, the method used is at variance with [16] and leads to an incorrect result for S-wave quarkonia produced through intermediate quark-antiquark pairs in a color octet P-wave state. In the following subsection we expound on the method discussed in [16] and hope to clarify this difference.

4.1 Polarized production

For arguments sake, let us consider the production of a ψ' in a polarization state λ. This state can be reached through quark-antiquark pairs in various spin and orbital angular momentum states, and we are led to consider the intermediate quark-antiquark pair as a coherent superposition of these states. Because of parity and charge conjugation symmetry, intermediate states with different spin S and angular momentum L can not interfere[¶], so that the only non-trivial situation occurs for ^3P_J-states, i.e. $S = 1$, $L = 1$.

In [9] it is assumed that intermediate states with different JJ_z, where J is total angular momentum do not interfere, so that the production cross section can be expressed as the sum over JJ_z of the amplitude squared for production of a color octet quark-antiquark pair in a $^3P_{JJ_z}$ state times the amplitude squared for its transition into the ψ'. The second factor can be inferred from spin symmetry to be a simple Clebsch-Gordon coefficient so that

$$\sigma_{\psi'}^{(\lambda)} \sim \sum_{JJ_z} \sigma(\bar{c}c[^3P_{JJ_z}^8]) \, |\langle JJ_z|1(J_z-\lambda);1\lambda\rangle|^2 \, . \tag{21}$$

We will show that this equation is incompatible with spin symmetry which requires interference of intermediate states with different J.

A simple check can be obtained by applying (21) to the calculation of the gluon fragmentation function into longitudinally polarized ψ'. Since the fragmentation functions into quark-antiquark pairs in a $^3P_{JJ_z}^8$ state follow from [28] by a change of color factor, the sum in (21) can be computed. The result not only differs from the fragmentation function obtained in [16] but contains an infrared divergence which can not be absorbed into another NRQCD matrix element.

To see the failure of (21) more clearly we return to the NRQCD factorization formalism. After Fierz rearrangement of color and spin indices as explained in [5], the cross section can be written as

$$\sigma^{(\lambda)} \sim H_{ai;bj} \cdot S_{ai;bj}^{(\lambda)} \, . \tag{22}$$

In this equation $H_{ai;bj}$ is the hard scattering cross section, and $S_{ai;bj}$ is the soft (non-perturbative) part that describes the 'hadronization' of the color octet quark pair into a ψ' plus light hadrons. Note that the statement of factorization entailed in this equation occurs only on the cross section and not on the amplitude level. The indices ij and ab refer to spin and angular

[¶]Technically, this means that NRQCD matrix elements with an odd number of derivatives or spin matrices vanish if the quarkonium is a C or P eigenstate.

momentum in a Cartesian basis $L_a S_i$ $(a, i = 1, 2, 3 = x, y, z)$. Since spin-orbit coupling is suppressed by v^2 in the NRQCD Lagrangian, L_z and S_z are good quantum numbers. In the specific situation we are considering, the soft part is simply given by (the notation follows [5, 16])

$$S^{(\lambda)}_{ai;bj} = \langle 0|\chi^\dagger \sigma_i T^A \left(-\frac{i}{2} \overleftrightarrow{D}_a\right) \psi \, a^{(\lambda)\dagger}_{\psi'} a^{(\lambda)}_{\psi'} \, \psi^\dagger \sigma_j T^A \left(-\frac{i}{2} \overleftrightarrow{D}_b\right) \chi|0\rangle \,, \tag{23}$$

where $a^{(\lambda)}_{\psi'}$ destroys a ψ' in an out-state with polarization λ. To evaluate this matrix element at leading order in v^2, we may use spin symmetry. Spin symmetry tells us that the spin of the ψ' is aligned with the spin of the $\bar{c}c$ pair, so $S^{(\lambda)}_{ai;bj} \propto \epsilon^{i*}(\lambda)\epsilon^j(\lambda)$. Now all vectors $S^{(\lambda)}_{ai;bj}$ can depend on have been utilized, and thus by rotational invariance, only the Kronecker symbol is left to tie up a and b. The overall normalization is determined by taking appropriate contractions, and we obtain

$$S^{(\lambda)}_{ai;bj} = \langle \mathcal{O}^{\psi'}_8 ({}^3P_0)\rangle \, \delta_{ab} \, \epsilon^{i*}(\lambda)\epsilon^j(\lambda) \,. \tag{24}$$

This decomposition tells us that to calculate the polarized production rate we should project the hard scattering amplitude onto states with definite $S_z = \lambda$ and L_z, square the amplitude, and then sum over L_z ($\sum_{L_z} \epsilon_a(L_z)\epsilon_b(L_z) = \delta_{ab}$ in the rest frame). In other words, the soft part is diagonal in the $L_z S_z$ basis.

It is straightforward to transform to the JJ_z basis. Since $J_z = L_z + S_z$, there is no interference between intermediate states with different J_z. To see this we write, in obvious notation,

$$\sigma^{(\lambda)} \sim \sum_{JJ_z;J'J'_z} H_{JJ_z;J'J'_z} \cdot S^{(\lambda)}_{JJ_z;J'J'_z} \,, \tag{25}$$

and using (24) obtain,

$$S^{(\lambda)}_{JJ_z;J'J'_z} = \langle \mathcal{O}^{\psi'}_8 ({}^3P_0)\rangle \sum_M \langle 1M;1\lambda|JJ_z\rangle\langle J'J'_z|1M;1\lambda\rangle \,, \tag{26}$$

which is diagonal in $(JJ_z)(J'J'_z)$ only after summation over λ (unpolarized production). In general, the off-diagonal matrix elements cause interference of the following JJ_z states: 00 with 20, 11 with 21 and $1(-1)$ with $2(-1)$. While the diagonal elements agree with (21), the off-diagonal ones are missed in (21).

To assess the degree of transverse ψ' (direct J/ψ) polarization at moderate p_t, the calculation of [9] should be redone with the correct angular momentum projections.

4.2 Polarization in fixed target experiments

Polarization measurements have been performed for both ψ [22] and ψ' [29] production in pion scattering fixed target experiments. Both experiments observe an essentially flat angular distribution in the decay $\psi \to \mu^+\mu^-$ $(\psi = J/\psi, \psi')$,

$$\frac{d\sigma}{d\cos\theta} \propto 1 + \alpha \cos^2\theta \,, \tag{27}$$

where the angle θ is defined as the angle between the three-momentum vector of the positively charged muon and the beam axis in the rest frame of the quarkonium. The observed values for α are 0.02 ± 0.14 for ψ', measured at $\sqrt{s} = 21.8\,\mathrm{GeV}$ in the region $x_F > 0.25$ and 0.028 ± 0.004 for J/ψ measured at $\sqrt{s} = 15.3\,\mathrm{GeV}$ in the region $x_F > 0$. In the CSM, the J/ψ's are predicted to be significantly transversely polarized [2], in conflict with experiment.

The polarization yield of color octet processes can be calculated along the lines of the previous subsection. We first concentrate on ψ' production and define ξ as the fraction of longitudinally polarized ψ'. It is related to α by

$$\alpha = \frac{1 - 3\xi}{1 + \xi}\,. \tag{28}$$

For the different intermediate quark-antiquark states we find the following ratios of longitudinal to transverse quarkonia:

$$\begin{array}{ccc} {}^3S_1^{(1)} & 1:3.35 & \xi = 0.23 \\ {}^1S_0^{(8)} & 1:2 & \xi = 1/3 \\ {}^3P_J^{(8)} & 1:6 & \xi = 1/7 \\ {}^3S_1^{(8)} & 0:1 & \xi = 0 \end{array} \tag{29}$$

where the number for the singlet process (first line) has been taken from [2][‖]. Let us add the following remarks:

(i) The ${}^3S_1^{(8)}$-subprocess yields pure transverse polarization. Its contribution to the total polarization is not large, because gluon-gluon fusion dominates the total rate.

(ii) For the ${}^3P_J^{(8)}$-subprocess J is not specified, because interference between intermediate states with different J could occur as discussed in the previous subsection. As it turns out, interference does in fact not occur at leading order in α_s, because the only non-vanishing short-distance amplitudes in the JJ_z basis are 00, 22 and $2(-2)$, which do not interfere.

(iii) The ${}^1S_0^{(8)}$-subprocess yields unpolarized quarkonia. This follows from the fact that the NRQCD matrix element is

$$\langle 0|\chi^\dagger T^A a_{\psi'}^{(\lambda)\dagger} a_{\psi'}^{(\lambda)}\, \psi^\dagger T^A \chi|0\rangle = \frac{1}{3}\,\langle \mathcal{O}_8^{\psi'}({}^1S_0)\rangle\,, \tag{30}$$

independent of the helicity state λ. At this point, we differ from [13], who assume that this channel results in pure transverse polarization, because the gluon in the chromomagnetic dipole transition ${}^1S_0^{(8)} \to {}^3S_1^{(8)} + g$ is assumed to be transverse. However, one should keep in mind that the soft gluon is off-shell and interacts with other partons with unit probability prior to hadronization. The NRQCD formalism applies only to inclusive quarkonium production. Eq. (30) then follows from rotational invariance.

(iv) Since the ${}^3P_J^{(8)}$ and ${}^1S_0^{(8)}$-subprocesses give different longitudinal polarization fractions, the ψ' polarization depends on a combination of the matrix elements $\langle \mathcal{O}_8^{\psi'}({}^1S_0)\rangle$ and $\langle \mathcal{O}_8^{\psi'}({}^3P_0)\rangle$ which is different from $\Delta_8(\psi')$.

To obtain the total polarization the various subprocesses have to be weighted by their partial cross sections. We define

[‖] This number is x_F-dependent and we have approximated it by a constant at low x_F, where the bulk data is obtained from. The polarization fractions for the octet $2 \to 2$ parton processes are x_F-independent.

$$\delta_8(H) = \frac{\langle \mathcal{O}_8^H({}^1S_0)\rangle}{\Delta_8(H)} \tag{31}$$

and obtain

$$\begin{aligned} \xi &= 0.23\,\frac{\sigma_{\psi'}({}^3S_1^{(1)})}{\sigma_{\psi'}} + \left[\frac{1}{3}\delta_8(\psi') + \frac{1}{7}(1-\delta_8(\psi'))\right]\frac{\sigma_{\psi'}({}^1S_0^{(8)} + {}^3P_J^{(8)})}{\sigma_{\psi'}} \\ &= 0.16 + 0.11\,\delta_8(\psi')\,, \end{aligned} \tag{32}$$

where the last line holds at $\sqrt{s} = 21.8\,\mathrm{GeV}$ (The energy dependence is mild and the above formula can be used with little error even at $\sqrt{s} = 40\,\mathrm{GeV}$). Since $0 < \delta_8(H) < 1$, we have $0.16 < \xi < 0.27$ and therefore

$$0.15 < \alpha < 0.44\,. \tag{33}$$

In quoting this range we do not attempt an estimate of $\delta_8(\psi')$. Note that taking the Tevatron and fixed target extractions of certain (and different) combinations of $\langle \mathcal{O}_8^{\psi'}({}^1S_0)\rangle$ and $\langle \mathcal{O}_8^{\psi'}({}^3P_0)\rangle$ seriously (see Sect. 5.1), a large value of $\delta_8(\psi')$ and therefore low α would be favored. Within large errors, such a scenario could be considered consistent with the measurement quoted earlier. From a theoretical point of view, however, the numerical violation of velocity counting rules implied by this scenario would be rather disturbing.

In contrast, the more accurate measurement of polarization for J/ψ leads to a clear discrepancy with theory. In this case, we have to incorporate the polarization inherited from decays of the higher charmonium states χ_{cJ} and ψ'. This task is simplified by observing that the contribution from χ_{c0} and χ_{c1} feed-down is (theoretically) small as is the octet contribution to the χ_{c2} production cross section. On the other hand, the gluon-gluon fusion process produces χ_{c2} states only in a helicity ± 2 level, so that the J/ψ in the subsequent radiative decay is completely transversely polarized. Weighting all subprocesses by their partial cross section and neglecting the small ψ' feed-down, we arrive at

$$\xi = 0.10 + 0.11\,\delta_8(J/\psi) \tag{34}$$

at $\sqrt{s} = 15.3\,\mathrm{GeV}$, again with mild energy dependence. This translates into sizeable transverse polarization

$$0.31 < \alpha < 0.63\,. \tag{35}$$

The discrepancy with data could be ameliorated if the observed number of χ_{c1} from feed-down were used instead of the theoretical value. However, we do not know the polarization yield of whatever mechanism is responsible for copious χ_{c1} production.

Thus, color octet mechanisms do not help to solve the polarization problem and one has to invoke a significant higher-twist contribution as discussed in [2]. To our knowledge, no specific mechanism has yet been proposed that would yield predominantly longitudinally polarized ψ' and J/ψ in the low x_F region which dominates the total production cross section. One might speculate that both the low χ_{c1}/χ_{c2} ratio and the large transverse polarization follow from

the assumption of transverse gluons in the gluon-gluon fusion process, as inherent to the leading-twist approximation. If gluons in the proton and pion have large intrinsic transverse momentum, as suggested by the p_t-spectrum in open charm production, one would be naturally led to higher-twist effects that obviate the helicity constraint on on-shell gluons.

5 Other processes

Direct J/ψ and ψ' production is sensitive to the color octet matrix element $\Delta_8(H)$ defined in (17). In this section we compare our extraction of $\Delta_8(H)$ with constraints from quarkonium production at the Tevatron and in photo-production at fixed target experiments and HERA.

5.1 Quarkonium production at large p_t

An extensive analysis of charmonium production data at $p_t > 5\,\mathrm{GeV}$ has been carried out by Cho and Leibovich [8, 9], who relaxed the fragmentation approximation employed earlier [6, 7]. At the lower p_t boundary, the theoretical prediction is dominated by the ${}^1S_0^{(8)}$ and ${}^3P_J^{(8)}$ subprocesses and the fit yields

$$\begin{aligned} \langle \mathcal{O}_8^{J/\psi}({}^1S_0)\rangle + \frac{3}{m_c^2}\langle \mathcal{O}_8^{J/\psi}({}^3P_0)\rangle &= 6.6\cdot 10^{-2} \\ \langle \mathcal{O}_8^{\psi'}({}^1S_0)\rangle + \frac{3}{m_c^2}\langle \mathcal{O}_8^{\psi'}({}^3P_0)\rangle &= 1.8\cdot 10^{-2}\,, \end{aligned} \tag{36}$$

to be compared with the fixed target values**

$$\begin{aligned} \langle \mathcal{O}_8^{J/\psi}({}^1S_0)\rangle + \frac{7}{m_c^2}\langle \mathcal{O}_8^{J/\psi}({}^3P_0)\rangle &= 3.0\cdot 10^{-2} \\ \langle \mathcal{O}_8^{\psi'}({}^1S_0)\rangle + \frac{7}{m_c^2}\langle \mathcal{O}_8^{\psi'}({}^3P_0)\rangle &= 0.5\cdot 10^{-2}\,. \end{aligned} \tag{37}$$

If we assume $\langle \mathcal{O}_8^{J/\psi}({}^1S_0)\rangle = \langle \mathcal{O}_8^{J/\psi}({}^3P_0)\rangle/m_c^2$, the fixed target values are a factor seven (four) smaller than the Tevatron values for J/ψ (ψ'). The discrepancy would be lower for the radical choice $\langle \mathcal{O}_8^{J/\psi}({}^3P_0)\rangle = 0$.

While this comparison looks like a flagrant violation of the supposed process-independence of NRQCD production matrix elements, there are at least two possibilities that could lead to systematic differences:

(i) The $2 \to 2$ color octet parton processes are schematically of the form

$$\frac{\langle \mathcal{O}\rangle}{2m_c}\,\frac{1}{M_f^2}\,\delta(x_1x_2s - M_f^2)\,, \tag{38}$$

** Since there is a strong correlation between the charm quark mass and the extracted NRQCD matrix elements, we emphasize that both (36) and (37) as well as (39) below have been obtained with the same $m_c = 1.5\,\mathrm{GeV}$ (or $m_c = 1.48$ GeV, to be precise). On the other hand, the apparent agreement of predictions for fixed target experiments with data claimed in [14] is obtained from (39) in conjunction with $m_c = 1.7\,\mathrm{GeV}$.

where M_f denotes the final state invariant mass. To leading order in v^2, we have $M_f = 2m_c$. Note, however, that this is physically unrealistic. Since color must be emitted from the quark pair in the octet state and neutralized by final-state interactions, the final state is a quarkonium accompanied by light hadrons with invariant mass squared of order $M_f^2 \approx (M_H + M_H v^2)^2$ since the soft gluon emission carries an energy of order $M_H v^2$, where M_H is the quarkonium mass. The kinematic effect of this difference in invariant mass is very large since the gluon distribution rises steeply at small x and reduces the cross section by at least a factor two. The 'true' matrix elements would therefore be larger than those extracted from fixed target experiments at leading order in NRQCD. Since the ψ' is heavier than the J/ψ, the effect is more pronounced for ψ', consistent with the larger disagreement with the Tevatron extraction for ψ'. Note that the effect is absent for large-p_t production, since in this case, $x_1 x_2 s > 4p_t^2 \gg M_f^2$. If we write $M_f = 2m_c + \mathcal{O}(v^2)$, then the difference between fixed target and large-p_t production stems from different behaviors of the velocity expansion in the two cases.

(ii) It is known that small-x effects increase the open bottom production cross section at the Tevatron as compared to collisions at lower $\sqrt{s}$. Since even at large p_t, the typical x is smaller at the Tevatron than in fixed target experiments, this effect would enhance the Tevatron prediction more than the fixed target prediction. The 'true' matrix elements would therefore be smaller than those extracted from the Tevatron in [9].

While a combination of both effects could well account for the apparently different NRQCD matrix elements, one must keep in mind that we have reason to suspect important higher twist effects for charmonium production at fixed target energies. Theoretical predictions for fixed target production are intrinsically less accurate than at large p_t, where higher-twist contributions due to the initial hadrons are expected to be suppressed by Λ_{QCD}/p_t (if not Λ_{QCD}^2/p_t^2) rather than Λ_{QCD}/m_c.

5.2 Photo-production

A comparison of photo-production with fixed target production is more direct since the same combination of NRQCD matrix elements is probed and the kinematics is similar. All analyses [10, 11, 12] find a substantial overestimate of the cross section if the octet matrix elements of (36) are used. The authors of [11] fit

$$\langle \mathcal{O}_8^{J/\psi}(^1S_0)\rangle + \frac{7}{m_c^2}\langle \mathcal{O}_8^{J/\psi}(^3P_0)\rangle \; = 2.0 \cdot 10^{-2}\,, \tag{39}$$

consistent with (37) within errors, which we have not specified. While this agreement is reassuring, it might also be partly accidental since the extraction of [11] is performed on the elastic peak, which is not described by NRQCD. Color octet mechanisms do not leave a clear signature in the total inelastic photo-production cross section. The authors of [10] argue that the color-octet contributions to the energy spectrum of J/ψ are in conflict with the observed energy dependence in the endpoint region $z > 0.7$, where $z = E_{J/\psi}/E_\gamma$ in the proton rest frame. This discrepancy would largely disappear if the smaller matrix element of (37) or (39) were used rather than (36). Furthermore, since in a color octet process soft gluons with energy $M_H v^2$ must be emitted, but are kinematically not accounted for, the NRQCD-prediction for the energy distribution should be smeared over an interval of size $\delta z \sim v^2 \sim 0.3$, making the steep rise of the energy distribution close to $z = 1$ is not necessarily physical.

6 Conclusion

We have reanalyzed charmonium production data from fixed target experiments, including color octet production mechanisms. Our conclusion is twofold: On one hand, the inclusion of color octet processes allows us to reproduce the overall normalization of the total production cross section with color octet matrix elements of the expected size (if not somewhat smaller) without having to invoke small values of the charm quark mass. This was found to be true for bottomonium as well as for charmonium. Comparing the theoretical predictions within this framework with the data implies the existence of additional bottomonium states below threshold which have not yet been seen directly.

On the other hand, the present picture of charmonium production at fixed target energies is far from perfect. The χ_{c1}/χ_{c2} production ratio remains almost an order of magnitude too low, and the transverse polarization fraction of the J/ψ and ψ' is too large. We thus confirm the expectation of [2] that higher twist effects must be substantial even after including the octet mechanism.

The uncertainties in the theoretical prediction at fixed target energies are substantial and preclude a straightforward test of universality of color octet matrix elements by comparison with quarkonium production at large transverse momentum. We have argued that small-x, as well as kinematic effects, could bias the extraction of these matrix elements in different directions at fixed target and collider energies. The large uncertainties involved, especially due to the charm quark mass, could hardly be eliminated by a laborious calculation of α_s-corrections to the production processes considered here. To more firmly establish existence of the octet mechanism there are several experimental measurements which need to be performed. Data on polarization is presently only available for charmonium production in pion-induced collisions. A measurement of polarization at large transverse momentum or for bottomonium is of crucial importance, because higher twist effects should be suppressed. Furthermore, a measurement of direct and indirect production fractions in the bottom system would provide further confirmation of the color octet picture and constrain the color octet matrix elements for bottomonium.

Acknowledgments. We thank S.J. Brodsky, E. Quack and V. Sharma for discussions. IZR acknowledges support from the DOE grant DE-FG03-90ER40546 and the NSF grant PHY-8958081.

References

[1] G.A. Schuler, 'Quarkonium production and decays', CERN report CERN-TH-7170-94 [hep-ph/9403387], and references therein

[2] M. Vänttinen, P. Hoyer, S.J. Brodsky and W.-K. Tang, Phys. Rev. **D51**, 3332 (1995)

[3] E. Braaten, M. Doncheski, S. Fleming and M. Mangano, Phys. Lett. **B333**, 548 (1994)

[4] D.P. Roy and K. Sridhar, Phys. Lett. **B339**, 141 (1994)

[5] G.T. Bodwin, E. Braaten and G.P. Lepage, Phys. Rev. **D51**, 1125 (1995)

[6] E. Braaten and S. Fleming, Phys. Rev. Lett. **74**, 3327 (1995)

[7] M. Cacciari, M. Greco, M.L. Mangano and A. Petrelli, Phys. Lett. **B356**, 553 (1995)

[8] P. Cho and A.K. Leibovich, Phys. Rev. **D53**, 150 (1996)

[9] P. Cho and A.K. Leibovich, CalTech report CALT-68-2026 [hep-ph/9511315]

[10] M. Cacciari and M. Krämer, DESY report DESY 96-005 [hep-ph/9601276]

[11] J. Amundson, S. Fleming and I. Maksymyk, University of Texas report UTTG-10-95 [hep-ph/9601298]

[12] P. Ko, J. Lee and H.S. Song, Seoul University report [hep-ph/9602223]

[13] W.-K. Tang and M. Vänttinen, SLAC report SLAC-PUB-95-6931 [hep-ph/9506378]; NORDITA report NORDITA-96/18 P [hep-ph/9603266]

[14] S. Gupta and K. Sridhar, Tata Institute report TIFR/TH/96-04 [hep-ph/9601349]

[15] P. Cho and M.B. Wise, Phys. Lett. **B346**, 129 (1995)

[16] M. Beneke and I.Z. Rothstein, University of Michigan report UM-TH-95-23 [hep-ph/9509375], to appear in Phys. Lett. **B**

[17] H. Jung, D. Krücker, C. Greub and D. Wyler, Z. Phys. **C60**, 721 (1993)

[18] F. Abe *et al.*, Phys. Rev. Lett. **75**, 4358 (1995)

[19] E. Eichten and C. Quigg, Phys. Rev. **D52**, 1726 (1995).

[20] H.L. Lai *et al.*, Phys. Rev. **D51**, 4763 (1995)

[21] M. Glück, E. Reya and A. Vogt, Z. Phys. **C53**, 651 (1992)

[22] C. Akerlof *et al.*, Phys. Rev. **D48**, 5067 (1993)

[23] M. H. Schub *et al.*, Phys. Rev. **D52**, 1307 (1995)

[24] T. Alexopoulos *et al.*, Fermilab report FERMILAB-Pub-95/297-E

[25] L. Antoniazzi *et al.*, Phys. Rev. Lett. **70**, 383 (1993)

[26] Y. Lemoigne *et al.*, Phys. Lett. **B113**, 509 (1982)

[27] D.M. Alde *et al.*, Phys. Rev. Lett. **66**, 2285 (1991)

[28] P. Cho, M.B. Wise and S. Trivedi, Phys. Rev. **D51**, 2039 (1995)

[29] J.G. Heinrich *et al.*, Phys. Rev. **D44**, 1909 (1991)